P H Y S I C A L   R E V I E W   L E T T E R S

Resonator-Aided Single-Atom Detection on a Microfabricated Chip

Igor Teper, Yu-Ju Lin, and Vladan Vuletić

MIT-Harvard Center for Ultracold Atoms, MIT, Cambridge, Massachusetts 02139, USA
(Received 23 March 2006; published 14 July 2006)

We use an optical cavity to detect single atoms magnetically trapped on an atom chip. We implement the detection using both fluorescence into the cavity and atom-induced reduction in cavity transmission. In fluorescence, we register 2.0(2) photon counts per atom, which allows us to detect single atoms with 75% efficiency in 250 μs. In absorption, we measure transmission attenuation of 3.3(3)% per atom, which allows us to count small numbers of atoms with a resolution of about 1 atom.

In the past several years, there have been many promising developments in the field of microfabricated magnetic traps (microtraps) for ultracold atoms, including experimental realizations of microtrap-based atom interferometers [1], atomic clocks [2], and Bragg reflectors [3]. Compared to optical traps, where significant progress in interferometry [4], Josephson junctions [5], and one-dimensional physics [6] has been made, microchips offer smaller length scales and tighter confinement for single traps, which, however, may require working with small atom numbers. Furthermore, there are many proposed atom chip experiments, such as the implementation of a Tonks-Girardeau gas [7–9] or an atomic Fabry-Perot interferometer [10] in a magnetic trap, that may greatly benefit from measuring atom statistics and correlations at the single-atom level, as has recently been demonstrated in a free-space experiment [11]. In addition, preparation and detection of single atoms in microtraps constitute an important step toward quantum information processing with neutral atoms, which could take advantage of the tight, complex, precisely controlled, and scalable magnetic traps available on microchips [12]. In this context, the problem arises of how to detect small atom numbers in magnetic microtraps close to a substrate surface with a good signal-to-noise ratio [13,14].

While cavity QED experiments [15] can detect and count single atoms in the strong coupling regime, integrating very high-finesse Fabry-Perot cavities with atom chips may prove difficult [14]. Observing small atom numbers through fluorescence in a magneto-optical trap (MOT) [16] or in MOT-loaded dipole traps [17] requires long measurement times, and is also not easily compatible with chip traps. While experimental progress has recently been made in incorporating fiber resonators [18] and microcavities [19] into atom chips, the capabilities of such detection methods remain to be established. Recently, a low-finesse concentric cavity was used for sensitive detection of atoms in a macroscopic magnetic waveguide in a free-space geometry [20].

Atom detection can be implemented via fluorescence [16,17] or absorption methods [11,15]. To compare the two

methods, consider a sample of a atoms, where each atom on average scatters m photons, and the imaging system detects a fraction α of the photons. If background counts can be neglected, the atom number uncertainty Δa_f in fluorescence detection is given by the ratio between the photon shot noise, $\sqrt{a\alpha m}$, and the signal per atom, αm, and is equal to $\Delta a_f = \sqrt{a/\alpha m}$. Consequently, in fluorescence measurements, the resolution decreases as the square root of the atom number.

For the equivalent linear-absorption measurement, we assume the same number m of scattered photons per atom with an absorption beam matched to the collection optics. Note that, for diffraction-limited collection optics, $\alpha = \sigma/(2\pi w^2)$ while the fraction of photons absorbed is $2\sigma/(\pi w^2) = 4\alpha$, where λ is the wavelength for the transition, w is the waist produced when a beam is coupled through the same optics, and $\sigma = 3\lambda^2/(2\pi)$ is the maximum atomic scattering cross section. Therefore, the number of incoming absorption-beam photons is $m/(4\alpha)$, with a corresponding shot noise $\sqrt{m/(4\alpha)}$. This results in an atom number uncertainty in absorption of $\Delta a_a = \sqrt{1/(4\alpha m)}$, similar to the fluorescence uncertainty for $a = 1$ but, unlike fluorescence, independent of atom number. Cavity-aided detection is attractive for both fluorescence and absorption methods, since the emission of light into the
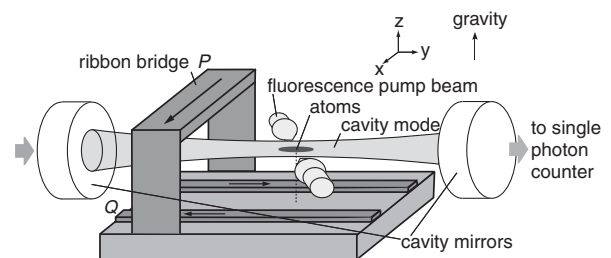

FIG. 1. Cavity and microfabricated chip (not to scale). The chip wires (Q) generate a 2D quadrupole field in the xz plane. The ribbon (P) combined with an external field gradient creates the confinement along y. Atoms are probed either with a pump beam from the side to induce fluorescence or through the absorption of a beam coupled through the cavity.

cavity is enhanced by the Purcell factor $2F/\pi$, where F is the cavity finesse [21].

In this Letter, we investigate the detection and counting of small numbers of atoms in a magnetic microtrap using a macroscopic, medium-finesse Fabry-Perot cavity employing both fluorescence and absorption techniques. Using shot-noise-limited atom preparation down to 1 atom, we achieve single-atom sensitivity in fluorescence, and a resolution of about 1 atom in absorption.

Our experimental setup (Fig. 1) is similar to that described in Ref. [22]. ^{87}Rb atoms are trapped and cooled in a magneto-optical trap and transferred to a magnetic trap, which is then adiabatically transformed into a Ioffe-Pritchard microtrap near the chip. The radial (xz) confinement of the chip trap is provided by two 2-μm-high, 500-μm-wide gold wires Q, whose centers are separated by 1 mm, carrying antiparallel currents along y, in superposition with a bias field along z. The axial (y) confinement is created by a current through a gold ribbon bridge P along x, 500 μm away from the chip's surface, in combination with an external field gradient along y.

High-reflectivity, low-loss mirrors mounted on opposite sides of the chip form a 2.66-cm-long near-confocal cavity with TEM$_{00}$ mode waist w of 56 μm (60 μm at atomic position), finesse $F = 8600$, linewidth $\kappa/(2\pi) = 650$ kHz, free spectral range of 5630 MHz, and transverse mode spacing of 230 MHz, aligned along the axis of our magnetic trap and located 200 μm away from the chip. The TEM$_{00}$ mode is matched to a single-mode fiber for spatial filtering of background light and coupled into a single-photon-counting module (SPCM). For the fluorescence measurement, a retroreflected pump beam with a waist of 250 μm illuminates the atoms at an angle of 70° to the cavity axis. We stabilize the cavity to an off-resonant laser using a Pound-Drever-Hall scheme, achieving a stability of 140 kHz/$\sqrt{10\ \text{kHz}}$ for a locked cavity, and <400 kHz frequency jitter in the several ms after the locking light is turned off, which is when we perform our measurements.

We initially load 10^5 atoms into a Ioffe-Pritchard microtrap located 200 μm from the surface, outside the cavity mode in order to prevent heating by the cavity-length stabilization light. We then use a fast radio frequency (rf) evaporation to remove all but a small number of cold atoms at a typical temperature of 15 μK. We ramp the magnetic field to move the trap into the cavity mode, turn off the locking light, and perform the fluorescence or absorption measurement. When located in the cavity, the magnetic trap has transverse and axial vibration frequencies around 300 and 50 Hz, respectively.

Both absorption and fluorescence signals in cavity-aided detection depend on the atoms' scattering rate of photons into the cavity. For an atom on the cavity axis, the fraction of photons scattered into each direction of the cavity is given by the single-atom cooperativity, $\eta = 6F/(\pi(wk)^2)$,

where $k = 2\pi/\lambda$; for us, $\lambda = 780$ nm and $\eta = 0.07$. To confirm our atom-cavity coupling experimentally, we measure the tuning of the transmission resonance by the atomic index of refraction for samples large enough that the atom number can be determined by standard absorption techniques. The tuning of the cavity resonance by N atoms well localized at the cavity waist is given by $\delta\nu = (\kappa/2) \times (\Gamma/\Delta)N\eta$, where Γ is the linewidth of the atomic transition and $\Delta \gg \Gamma$ is the detuning between the laser and the atomic transition. This measurement of $\delta\nu$ yields a value of η between 0.015 and 0.025, in good agreement with the value we would expect given our independent measurement of the cloud size, which reduces η compared to the on-axis case.

To characterize both the atom number preparation and the number of photon counts per atom in fluorescence detection, we illuminate the atoms with a pump beam resonant with the $5^2S_{1/2}$, $F = 2 \rightarrow 5^2P_{3/2}$, $F = 3$ transition just above saturation and count the photons emerging from the cavity within 750 μs. We compile histograms of counts for different rf final settings, i.e., different average numbers of prepared atoms. Given that the photons emitted by each atom obey Poisson statistics, the following relation can be derived: $\langle n^2 \rangle / \langle n \rangle - 1 = g_{aa}\langle n \rangle + \langle p \rangle$, where $\langle a \rangle$ is the mean atom number, $\langle p \rangle$ is the mean number of photon counts per atom, $n = ap$ is the number of signal photon counts, and $g_{aa} = (\langle a^2 \rangle - \langle a \rangle)/\langle a \rangle^2$ is the atom-atom correlation function, which should be equal to 1 if the atoms obey Poisson statistics and equal to $(1 + f^2)$ in the presence of (technical) fractional atom number noise of magnitude f. The values of $\langle n^2 \rangle / \langle n \rangle - 1$ can be computed from each histogram independently without any knowledge about $\langle a \rangle$ or $\langle p \rangle$, given that we can measure the background count rate independently, and assuming that the background is uncorrelated with the signal. The results, along with a linear fit, are plotted in Fig. 2. The fit gives a slope of $g_{aa} = 1.05(2)$, which implies that the fractional noise on our signal is 0.25(10), and therefore Poissonian fluctuations dominate for the atom numbers we measure, and an intercept of $\langle p \rangle = 1.9(3)$ photon counts per atom.
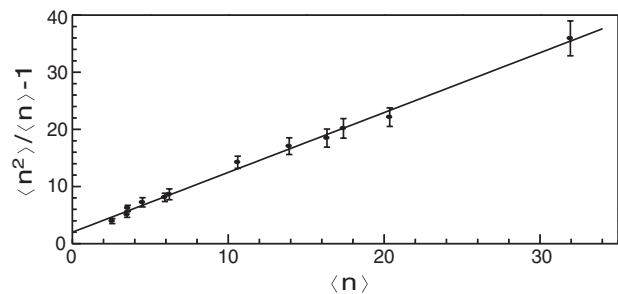

FIG. 2. Characterization of atom number fluctuations and detected photons per atom for fluorescence detection. n is the number of signal photons detected. The slope gives the atom-atom correlation function, g_{aa}, and the y-axis intercept gives the average number of photon counts per atom, $\langle p \rangle$.

Having confirmed the Poisson statistics of our atom number preparation, we can fit $\langle a \rangle$ and $\langle p \rangle$ for each histogram individually, assuming a Poisson distribution of atoms with mean $\langle a \rangle$, each of which emits a Poisson distribution of photons of which we detect a mean of $\langle p \rangle$. A typical histogram with fit and a plot of the combined results of all histogram fits are shown in Fig. 3. To a good approximation, the average number of photon counts per atom is independent of atom number at $\langle p \rangle = 2.0(2)$ counts/atom, with 0.3 background counts. An average of the signal time traces yields a $1/e$ time of $\tau = 150 \ \mu s$, likely limited by the atoms' being pushed out of the cavity mode due to a small imbalance between the intensities of the original and retroreflected pump beams.

Since our cavity resonance is much narrower than the atomic line, the cavity collects predominantly the coherently scattered photons. The number of photon counts we would expect to detect per atom is thus given by $\langle p \rangle = \Gamma_{coh} \tau \eta (\kappa/\gamma) C_+ g f q l$, where $\Gamma_{coh} = \Gamma/8 = 2\pi \times 760$ kHz is the maximum coherent scattering rate for the transition, $\eta = 0.07$, $\gamma = 2\pi \times 1$ MHz is the linewidth of the cavity transmission, which is a convolution of the cavity and laser linewidths, $C_+ = 0.3$ is the averaged Clebsch-Gordan coefficient for σ^+ intracavity light coming from the scattering process (the other polarizations are not resonant with the cavity), $g = 0.6$ accounts for the finite size of the atomic cloud, $f = 0.7$ is the coupling efficiency into the single-mode fiber, $q = 0.58$ is the quantum efficiency of the SPCM, and $l = 0.7$ is the signal reduction due to mechanical cavity vibrations measured independently via cavity transmission. The combination of the above factors predicts $\langle p \rangle = 1.7$, close to our measured value.

In order to quantify our fluorescence measurement as a single-atom detector, we reduce the measurement window to 250 μs, and take a histogram with, on average, less than one atom prepared. The Poisson fit to the resulting histogram gives $\langle a \rangle = 0.85(8)$ and $\langle p \rangle = 1.4(1)$. Combined with a measured background of 0.07 counts, this means that, if we set our detection threshold to ≥ 1 count, our single-atom detection is characterized by an atom quantum efficiency of 75% and a false detection rate of 7%, at a maximum single-atom count rate of 4 kHz.

While the fluorescence measurement makes a good single-atom detector, we expect an absorption measurement to provide better atom number resolution for $a > 1$. For absorption detection, we couple the probe laser beam into the cavity TEM$_{00}$ mode and monitor the resonant transmission through the cavity in the presence of atoms. The laser linewidth is broadened by frequency modulation to 30 MHz, much wider than κ, so that the intensity noise on the cavity transmission due to cavity vibration is negligible compared to the photon shot noise. The laser is tuned to atomic resonance with an intracavity saturation parameter equal to 0.2, which for one atom should result in transmission reduction of 2η. Similarly to fluorescence detection, we compile histograms collected in 1 ms for different atom preparation parameters and fit them, assuming Poisson statistics for both the atoms and the photons per atom, to determine the mean absorption per atom, $\langle s \rangle$, and the mean atom number, $\langle a \rangle$. [The signal lasts for a $1/e$ time of 560 μs, and a correlation function fit similar to the one for fluorescence confirms that our atom preparation for absorption has Poisson statistics, with $g_{aa} = 0.94(4)$.] The fitting results for $\langle s \rangle$ with varying atom number are shown in Fig. 4. From these measurements, we obtain $\langle s \rangle = 3.3(3)\%$, in good agreement with the expected absorption per atom, $\langle s \rangle = 3.2(7)\%$, when geometric factors due to finite cloud size are taken into account.

Using the measured values of $\langle p \rangle = 2.0(2)$ counts/atom for fluorescence and $\langle s \rangle = 3.3(3)\%$ for absorption, we can evaluate how well these two methods can determine the atom number in a single measurement. The expected atom number uncertainty δa using fluorescence (absorption) detection due to both photon shot noise and the statistical uncertainty in the mean number of photons per atom, $\langle p \rangle$ (uncertainty in the mean absorption per atom, $\langle s \rangle$), as well as the background photon counts (for fluorescence only), is plotted as a function of atom number in Fig. 5; the figure also includes a computed normalized histogram that characterizes the single-atom detection capability of our fluorescence measurement. For fluorescence, the atom number resolution is limited by the shot noise of the collected signal photons, which grows with atom number, while,
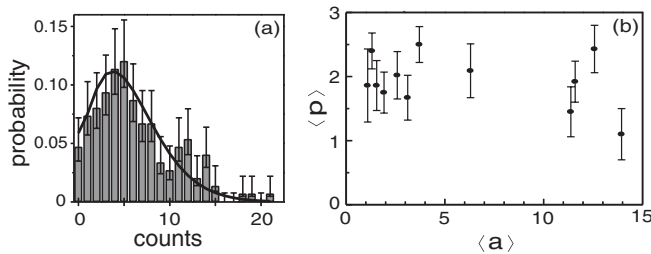

FIG. 3. (a) Typical normalized histogram of 150 fluorescence measurements, with Poisson fit to $\langle a \rangle$, the mean number of atoms, and $\langle p \rangle$, the mean number of photon counts per atom [here, $\langle a \rangle = 3.1(4)$ and $\langle p \rangle = 1.7(3)$]. Error bars are Poisson uncertainties. (b) Results of such fits to 12 different histograms; error bars correspond to 1 standard deviation in $\langle p \rangle$.
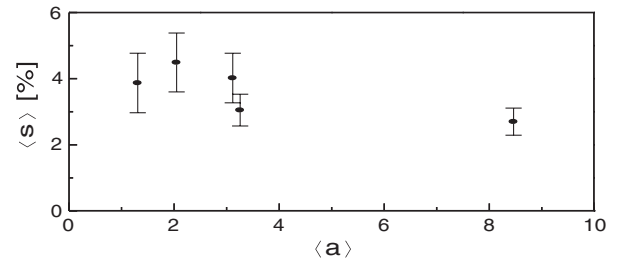

FIG. 4. Results of Poisson fits to $\langle s \rangle$, the mean single-atom absorption, and $\langle a \rangle$, the mean atom number, for 5 different histograms.
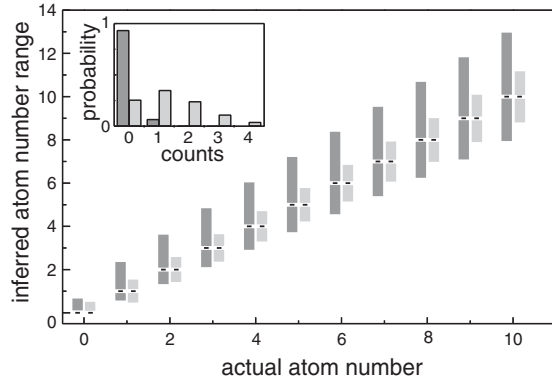
FIG. 5.   Single-shot atom number measurement 1-σ confidence intervals for fluorescence ($t = 750\ \mu$s, dark gray) and absorption ($t = 1$ ms, light gray). The inset shows computed normalized photon count distributions due to background counts (dark gray) and to photons collected from one atom (light gray) for fluorescence single-atom detection ($t = 250\ \mu$s).

for absorption, where the number of collected photons actually decreases with atom number, the resolution remains nearly flat, at around 1 atom.

The demonstrated excellent atom number resolution could be useful in a variety of microchip experiments. For instance, a Tonks-Girardeau (TG) gas could be created close to the chip, at high radial vibration frequencies, and then moved into the cavity to measure both the atom number and the density distribution of the gas. A quantum degenerate gas of 50 ^{87}Rb atoms confined in a magnetic trap with a radial trapping frequency of 20 kHz and an axial frequency of 0.5 Hz would be deep in the TG regime, with $\gamma = 2/(n|a_{1D}|)$ of 10, where $\gamma \gg 1$ means strong fermionization, for a peak one-dimensional number density n and an effective one-dimensional scattering length a_{1D} [8]. Then the spatial (30 μm) and atom number resolution of our detector would allow one to distinguish the length and density distribution of this TG gas ($l = 300\ \mu$m) from a corresponding nonfermionized Thomas-Fermi gas ($l = 420\ \mu$m).

In conclusion, we have demonstrated *in situ* detection of magnetically trapped atoms on a chip with the aid of a medium-finesse macroscopic cavity and characterized the performance for single-atom detection and for atom number measurements using both fluorescence and absorption methods. We believe that, due to their combination of versatility, performance, and ease of use, such cavity-aided detection schemes can play an important role in a broad range of applications in integrated atom optics on chips.

[1] Y.-J. Wang, D. Z. Anderson, V. M. Bright, E. A. Cornell, Q. Diot, T. Kishimoto, M. Prentiss, R. A. Saravanan, S. R. Segal, and S. Wu, Phys. Rev. Lett. **94**, 090405 (2005); T. Schumm, S. Hofferberth, L. M. Andersson, S. Wildermuth, S. Groth, I. Bar-Joseph, J. Schmiedmayer, and P. Krüger, Nature Phys. **1**, 57 (2005).

[2] P. Treutlein, P. Hommelhoff, T. Steinmetz, T. W. Hänsch, and J. Reichel, Phys. Rev. Lett. **92**, 203005 (2004).

[3] A. Günther, S. Kraft, M. Kemmler, D. Koelle, R. Kleiner, C. Zimmermann, and J. Fortágh, Phys. Rev. Lett. **95**, 170405 (2005).

[4] Y. Shin, M. Saba, T. A. Pasquini, W. Ketterle, D. E. Pritchard, and A. E. Leanhardt, Phys. Rev. Lett. **92**, 050405 (2004).

[5] M. Albiez, R. Gati, J. Fölling, S. Hunsmann, M. Cristiani, and M. K. Oberthaler, Phys. Rev. Lett. **95**, 010402 (2005).

[6] B. L. Tolra, K. M. O'Hara, J. H. Huckans, W. D. Phillips, S. L. Rolston, and J. V. Porto, Phys. Rev. Lett. **92**, 190401 (2004); B. Paredes, A. Widera, V. Murg, O. Mandel, S. Fölling, I. Cirac, G. V. Shlyapnikov, T. W. Hänsch, and I. Bloch, Nature (London) **429**, 277 (2004); T. Kinoshita, T. Wenger, and D. S. Weiss, Phys. Rev. Lett. **95**, 190406 (2005).

[7] M. Olshanii, Phys. Rev. Lett. **81**, 938 (1998).

[8] V. Dunjko, V. Lorent, and M. Olshanii, Phys. Rev. Lett. **86**, 5413 (2001).

[9] J. Reichel and J. H. Thywissen, J. Phys. IV **116**, 265 (2004).

[10] I. Carusotto, Phys. Rev. A **63**, 023610 (2001).

[11] A. Öttl, S. Ritter, M. Köhl, and T. Esslinger, Phys. Rev. Lett. **95**, 090404 (2005).

[12] T. Calarco, E. A. Hinds, D. Jaksch, J. Schmiedmayer, J. I. Cirac, and P. Zoller, Phys. Rev. A **61**, 022304 (2000).

[13] P. Horak, B. G. Klappauf, A. Haase, R. Folman, J. Schmiedmayer, P. Domokos, and E. A. Hinds, Phys. Rev. A **67**, 043806 (2003).

[14] R. Long, T. Steinmetz, P. Hommelhoff, W. Hänsel, T. W. Hänsch, and J. Reichel, Phil. Trans. R. Soc. A **361**, 1375 (2003).

[15] P. Münstermann, T. Fischer, P. W. H. Pinkse, and G. Rempe, Opt. Commun. **159**, 63 (1999); J. McKeever, J. R. Buck, A. D. Boozer, and H. J. Kimble, Phys. Rev. Lett. **93**, 143601 (2004).

[16] C.-S. Chuu, F. Schreck, T. P. Meyrath, J. L. Hanssen, G. N. Price, and M. G. Raizen, Phys. Rev. Lett. **95**, 260403 (2005).

[17] N. Schlosser, G. Reymond, I. Protsenko, and P. Grangier, Nature (London) **411**, 1024 (2001); S. Kuhr, W. Alt, D. Schrader, M. Müller, V. Gomer, and D. Meschede, Science **293**, 278 (2001).

[18] P. A. Quinto-Su, M. Tscherneck, M. Holmes, and N. P. Bigelow, Opt. Express **12**, 5098 (2004).

[19] M. Trupke, E. A. Hinds, S. Eriksson, E. A. Curtis, Z. Moktadir, E. Kukharenka, and M. Kraft, Appl. Phys. Lett. **87**, 211106 (2005).

[20] A. Haase, B. Hessmo, and J. Schmiedmayer, Opt. Lett. **31**, 268 (2006).

[21] E. M. Purcell, Phys. Rev. **69**, 681 (1946).

[22] Y. Lin, I. Teper, C. Chin, and V. Vuletić, Phys. Rev. Lett. **92**, 050404 (2004).